GALILEO GALILEI (GG)

PHASE A2 STUDY
EXECUTIVE SUMMARY

DRL/DRD: DEL-14

Written by	***Responsibility***
A. ANSELMI	Author
Verified by	
n.a.	Checker
Approved by	
	Product Assurance
	Configuration Control
	Design Engineer
	System Engineering Manager
A. ANSELMI	Study Manager
Documentation Manager	
R. Cavaglià	

The validations evidence are kept through the documentation management system.

ISSUE	DATE	§ CHANGE RECORDS	AUTHOR
01	8-Jun-09	First issue submitted to Preliminary Requirements Review	AA

TABLE OF CONTENTS

1. BACKGROUND

GG is a small satellite which aims at testing the Equivalence Principle to 1 part in 10^{17}. It would improve by 4 orders of magnitude the best ground based laboratory tests as well as those based on Lunar Laser Ranging.

The Equivalence Principle is the founding pillar of General Relativity and testing it to very high accuracy is widely recognized as a crucial asset for fundamental physics beyond the Standard Model of particle physics. The open problems of modern Cosmology − from dark matter to dark energy − all point to the need of putting General Relativity to the most stringent possible tests.

The current state of the art of the Universality of Free Fall experiments bases on ground experiments. $\eta=10^{-12}$ was achieved with rotating torsion balances at the University of Washington in Seattle, US (recently, an improvement to about 10^{-13} was announced). Lunar Laser Ranging provided a test to 10^{-13} for the Earth and the Moon in the gravitational field of the Sun.

It has been long recognized that only an experiment in space will provide optimal conditions for testing the Equivalence Principle to very high accuracy. As compared to test masses in free-fall towers, the experiment can last as long as the satellite keeps orbiting the Earth. As compared to test masses suspended on torsion balances in the lab, the driving signal in space is about 3 orders of magnitude stronger. In space, absence of weight allows the test masses to be suspended from the spacecraft much more gently than on ground; they are close to free test masses, and therefore they can be proportionally more sensitive to external effects. Finally, the orbiting spacecraft enclosing the instrument is an isolated system. Hence the perturbing effects of a laboratory experiment (terrain tilts and seismic noise; motor and bearings noise; nearby mass anomalies not rotating with the instrument) are utterly absent.

Two major space EP experiments, besides GG, have been proposed.

NASA has been the first space agency to support an experiment to test the Equivalence Principle in space. That experiment, STEP (Satellite Test of the Equivalence Principle), proposed by Stanford University, is still under investigation. It was studied by ESA too, in collaboration with NASA, in the 1990's. STEP features a cryogenic payload, a large total mass (1 ton at launch) and the goal of reaching 10^{-18}. Today NASA has no firm plans for flying STEP.

CNES, with support from ESA, is completing construction of the *Microscope* satellite, with the goal of performing an EP test to 10^{-15} (room temperature experiment, about 300 kg total mass at launch). The launch is currently expected to take place in 2011 (the final decision has been delayed by the immature status of the micropropulsion, now being resolved).

GG targets an EP test to 10^{-17}, without cryogenics, by a new instrument concept designed and optimized for this purpose. Avoiding the need for cryogenics makes the GG satellite small and low cost, probably the only world class experiment that is in the scope of a small satellite mission. Since it requires a low Earth equatorial orbit, GG can be launched by the European medium launcher VEGA and operated from the ASI station in Malindi.

ASI was first made aware of GG in 1996, when ESA declared its intention to provide financial support to a national mission devoted to testing the Equivalence Principle. At the time GG was a novel concept and it was not possible to provide sufficient experimental evidence. Soon afterwards GG was selected as candidate in the first competition for a small satellite mission of ASI. This led to the first industrial study of the satellite mission, at Phase A level, performed in 1997-98 by Alenia Spazio [RD 1].

GG was not selected in that competition. Later, ASI funded an additional study, in order to investigate the possibility to run the GG experiment in a high inclination sun synchronous orbit, for which cheaper launchers were available [RD 2].

Subsequently, INFN became interested in GG and, after thorough review of the experiment concept, funded a dedicated laboratory for a full scale prototype of the GG payload (GG on the Ground-GGG). The GGG national experiment of INFN has provided increasing experimental evidence and constantly improving sensitivity, even in the hostile ground environment.

Due to these scientific results, and thanks to the support of the Italian Cosmology community, GG was included in the 2006-2008 *Piano Spaziale Nazionale* of ASI. This led to a new industrial study, Phase A2, awarded by ASI to ThalesAlenia Space–Italy (TAS-I), the subject of this document.

The objectives of this study included a new review of the experiment concept in the light of the GGG lab experience, updated and improved definition of the payload and the spacecraft, with particular regard to the enabling technologies, updated mission and control design, and a thorough bottom-up cost estimate including, for the first time, the ground segment.

The Phase A2 industrial study was carried out between September 2008 and June 2009, under the direction of ASI, by a team led by ThalesAlenia Space (Torino) and including the TAS-I centers in Milano and Firenze, DTM Technologies, ALTA, and ALTEC, INRIM and the Polytechnic of Torino. The study progressed in tight collaboration with the PI and her team at the University of PISA/INFN, who were conducting a parallel contract on an improved version of the GGG lab experiment. The study went through two intermediate reviews and ended with a Preliminary Requirements Review, to which about 30 documents were submitted, including specifications, plans, design reports and technology assessments, a risk analysis, and a cost report. The achievements of the study include a high fidelity software simulator, developed after the blueprint of the GOCE simulator, which today (late Spring 2009) is proving its worth in the commissioning of the GOCE satellite, and a proven Spin Rate Sensor breadboard.

As a result of the Phase A2 study, the GG project is mature for an immediate start of the Implementation Phase, should this be the decision of ASI.

2. EXPERIMENT CONCEPT AND PAYLOAD DESIGN

2.1 Experiment Concept

Two test masses of different composition form the GG differential accelerometer. The test masses are heavy (10 kg each) concentric, co-axial, hollow cylinders. The two masses are mechanically coupled by attaching them at their top and bottom to two ends of a coupling arm, using soft springs. The coupling arm is made of two concentric tubes similarly attached at their midpoints to a single shaft. This assembly preserves the overall symmetry of the apparatus, when the two parts of the arm are taken together.

The masses are mechanically coupled through the balance arm such that they are free to move in the transverse (XY) plane. Differential acceleration acting on the masses gives rise to a displacement of the equilibrium position in the XY plane. The displacement of the test masses is sensed by two sets of capacitance plates located between the test cylinders, one set for each orthogonal direction (X and Y). Each set forms an AC-bridge so that a displacement of the masses causes an unbalance of the bridge and is converted into a voltage signal. When the physical system is mechanically well balanced, it is insensitive to `common-mode' accelerations. Moreover, the capacitance bridges are inherently sensitive to differential displacements. Thus, the differential nature of the accelerometer is ensured both by the dynamics of the physical system, and by the displacement transducer.

Testing the EP to 1 part in 10^{17} in the gravitational field of the Earth at 600-700 km altitude requires detection of a differential acceleration $a_{EP} \approx 8 \cdot 10^{-17}$ m/s^2. To achieve this sensitivity, the test masses must be very weakly coupled, otherwise the displacement signal resulting from such tiny acceleration is too small to detect. Moreover, the signal (at the orbital frequency) must be up-converted to higher frequency, the higher the better, to reduce 1/f noise.

In the GG accelerometer, the natural period of the differential mode will be designed to be about 545s. At that natural frequency, the EP acceleration signal a_{EP} will produce a displacement $\Delta x_{EP} \approx 0.6$ pm in the direction of the centre of the Earth. By spinning the satellite and the accelerometer, with its displacement transducer, around their common symmetry axis, the EP violation displacement signal is modulated at the spin frequency of the system relative to the centre of the Earth.

Once in orbit, the spacecraft will be given the required rate of rotation (1 Hz with respect to the centre of the Earth). All parts of the apparatus and the satellite co-rotate around a common symmetry axis. Spin speed is chosen to optimize the stability of the experiment and satellite. Due to the very weak coupling between the masses and rapid spin, the GG system is a rotor in supercritical regime and supercritical rotors are known to be self-centering even if fabrication and mounting errors give rise to departures from ideal cylindrical symmetry. Moreover, the spacecraft too is passively stabilized by rotation around its symmetry axis and no active attitude control is required for the entire duration of the space mission.

The only disadvantage of spinning at frequencies above the natural oscillation frequencies of the rotor is the onset of whirl motions. These occur at the natural frequencies of the system as “orbital” motion of the masses around their equilibrium position. Whirl arises due to energy losses in the suspensions: the smaller the losses, the slower the growth rate of whirl. It must be damped to prevent instability. Provided the quality factor Q of the suspensions is at least 20,000 (which laboratory tests have shown to be achievable), whirl growth is so slow that experiment runs can be performed between successive damping cycles, thus avoiding any disturbance from damping forces.

The largest disturbing accelerations experienced by the accelerometer are due to residual air drag and other non-gravitational forces such as sun and Earth radiation pressure. Such inertial accelerations act on the spacecraft and not on test masses suspended inside it, and are, in principle, the same on both the test bodies. Ideally, common mode effects do not produce any differential signal; in reality, they can only be partially rejected. The approach taken in GG calls for surface accelerations to be partially compensated by a drag free control system, and partially abated by the accelerometer's own common-mode rejection. Drag compensation requires the spacecraft to be equipped with proportional thrusters and a control system to force the spacecraft to follow the motion of an undisturbed test mass inside it at (and close to) the frequency of the signal.

Another potential threat is due to temperature effects. Temperature differences can give rise to differential accelerations via (a) the "radiometer effect", (b) differential elongation of the coupling arms, (c) differential changes in the stiffness of the suspensions, (d) expansion of the test masses leading to change of their position w.r.t. the capacitance sensors. The temperature requirements call for 0.2°C/day test mass temperature stability; 1°C axial gradient across the test bodies and the coupling arms. Such performance, which was shown feasible by passive thermal insulation alone, allows 20 days of data taking before rebalancing the test bodies, and at least 15 days before rebalancing the read-out capacitance bridge.

A detailed analysis of the experiment requirements was carried out in Phase A2 and is documented in a preliminary experiment requirements specification [RD 6], published as an addendum to the mission requirements [RD 8].

2.2 Payload Design

The GG payload is constituted by the PGB (Pico Gravity Box) laboratory, enclosing (Figure 2.2-1):

- The two cylindrical test masses
- Capacitance plates for "science-level" sensing of test mass relative displacements
- Small capacitance sensors/actuators for sensing relative displacements and damping the whirl motions
- Suspension springs and coupling elements
- Inchworms and piezo-ceramics for fine mechanical balancing and calibration
- Launch-lock mechanisms, associated to all suspended bodies.

The PGB also carries a small mirror, in correspondence of a photo-detector mounted on the inner surface of the spacecraft, for measuring small residual phase lags with respect to the spacecraft.

The payload electronics include:

- The PGB Control and Processing Electronics (CPE), located on the spacecraft platform, managing PGB motion control (whirl sensing, whirl damping and drag-free control) and processing of all signals coming from the test masses (motion control and EP sensing).
- The Experiment Control Electronics (ECE), housed inside the PGB, and communicating with the CPE via an optical link. The ECE locally manages whirl sensing and damper activation, under control by the CPE processor, and readout of the EP chain.

The payload apparatus further includes the necessary electrical harness and connectors and the thermal insulation.

Notable innovations w.r.t. the payload design addressed previously, which have evolved in this Phase A2 study, include the following.

- With respect to the 2003 status [RD 2], the configuration has moved back from the 2-accelerometer (i.e., 4 test masses) design to the simpler single-accelerometer design.
- With respect to the 1998 status [RD 1], the design of the mechanical suspensions has been improved (replacement of flat gimbals and helical springs with U-shaped suspensions; part of the suspension is now rigidly connected to the test masses).
- For the first time, a detailed, hierarchical specification of the experiment requirements was undertaken [RD 6].
- The test mass materials were addressed for technological feasibility as well as scientific performance. The current choice is for a Tungsten alloy for the heavier inner test mass and high density polyethylene (HDPE) for the lighter outer test mass. The dimensions and inertia properties of the test masses themselves were adapted to reflect the selected materials and the applicable requirements [RD 4].
- Potential plasma induced charging effects on the PGB and their countermeasures were addressed. As an outcome of this analysis, it was decided to place a positively polarized grid (repelling the ions) at the PGB inlet (open to allow outgassing).
- Potential magnetic effects on the PGB were assessed, to be damped by wrapping the PGB in a mu-metal shield.
- The configuration of the experiment was modeled in all details, basing on the current configuration of the laboratory experiment (Figure 2.2-1). All properties assumed in the spacecraft models are now firmly based on experimental laboratory evidence.
- The mechanism for passive compensation of the expansion/contraction of the spacecraft, envisaged in the 1998 study, was removed, as it was shown that the effect can be kept small by design, and the rest compensated by the DFACS [RD 16].
- The launch lock mechanisms were designed basing, among others, on the experience gained in similar tasks in the Lisa Pathfinder project (Figure 2.2-2).

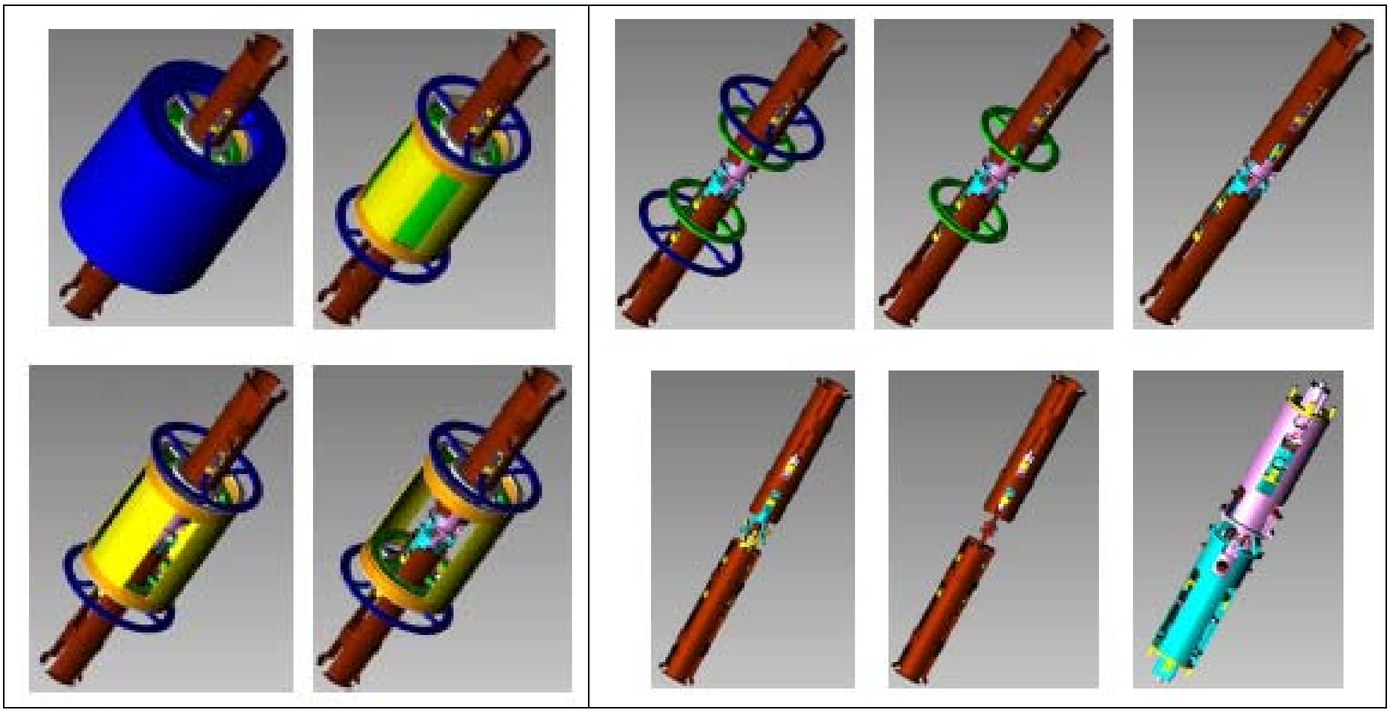

Figure 2.2-1: Details from the engineering drawings of the GG differential accelerometer.

The figures disclose the component parts by going further and further from the outside to the inside. (Left) The brown central tube is the PGB shaft. The blue and green cylinders are the test cylinders; the yellow plates are the capacitance bridge plates to measure the relative displacements of the test cylinders. The outer diameter of the blue test cylinders is about 23 cm. (Right) In the last picture only the coupling arm remains, and it is clear how it is made symmetric by putting together the two parts (pink and light blue). In the figure before the last, the PGB shaft is well visible, showing its center where the two pieces of the coupling are connected, each one with 3 U shaped laminar suspensions at 120° from each other.

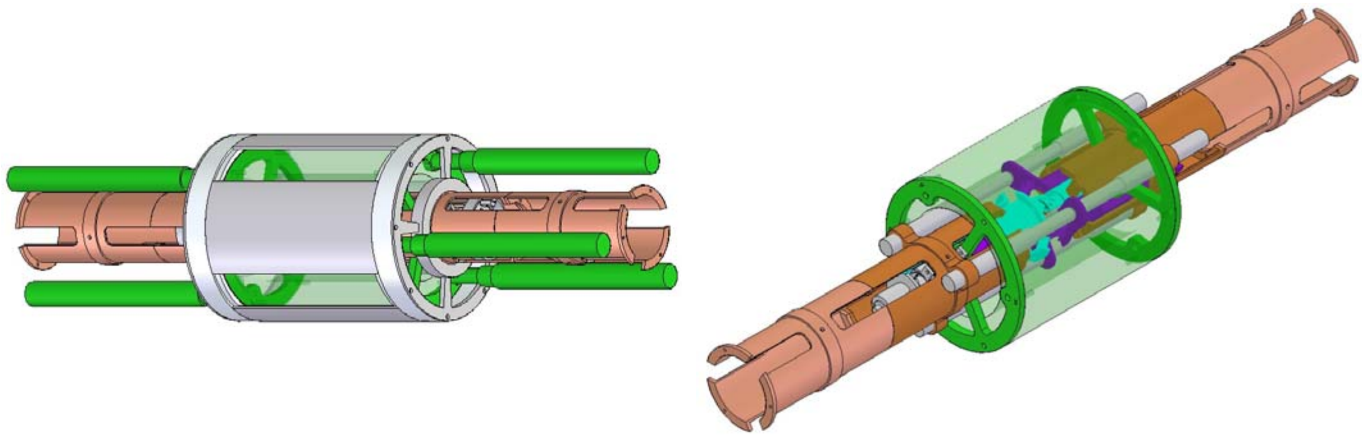

Test mass launch lock | Inner differential measuring devices lock

Figure 2.2-2: Design of the launch lock mechanisms.

3. MISSION DESIGN

The GG mission is devoted to a single experiment that, once initialized, runs to the end of the scientific data collection. After the launch and early orbit phase, experiment set-up and first calibration operations are executed. Thereafter, the experiment is run in 7-day long data collection intervals. Calibration sessions are regularly interspersed with the measurement intervals. Continuation of the mission improves the measurement accuracy with the square root of the measurement time. The nominal duration of the mission is 1 year plus 1 year optional extension.

No orbital change maneuvers are required after acquisition of the operational orbit, approximately 1.5 hours after lift-off. The processing of scientific data is done in bulk; therefore no scientific quick-look is required. All scientific operations are autonomous, executed on the basis of time-tagged operation sequences that are loaded at least one day in advance. Given the high level of autonomy, the tasks of the ground control are essentially limited to:

- Commanding and monitoring of the attitude maneuvers (initial spin axis orientation and spin-up)
- Generation and transmission of command sequences and parameters
- Analysis of satellite data to establish that the satellite is operating correctly.

The mission is performed in equatorial circular orbit. The dedicated ground station is San Marco, Malindi, Kenya. The satellite will be launched directly into near-circular, near-equatorial orbit by a small / medium launcher such as Vega (baseline) or PSLV (backup). Both launchers have capability much in excess of a small spacecraft such as GG [RD 22].

The design launch altitude will be between 500 km and 700 km, according to the strategy shown in Figure 2.2-1. No orbit maintenance is planned, and the spacecraft altitude will be allowed to decay gently in time, with negligible impact on the satellite mission and operations.

In the science measurements phase, the operation will be essentially autonomous. The Normal Mode is characterized by the drag-free control, executed by proportional microthrusters. However, the survival of the mission does not depend on the drag-free control, since the maintenance of the operational attitude is guaranteed by the gyroscopic stability. In case of malfunctions, the scientific operations will be put on hold and housekeeping data will be collected and transmitted to ground on the next station passes; resumption of the operations will be commanded by the ground.

The scientific data comprise the position of the test masses relative to each other and the “laboratory” (PGB), the time, the spin reference signal and ancillary data such as the temperature, the attitude of the spin axis and the phase difference between the PGB and the spacecraft’s outer vessel. The scientific data collection rate is small, about 20 kbit/s, and the total telemetry rate is well below the limit data rate (1 Mbps) of the ESA S-band ground stations, including Malindi, even in the worst case of 12-hour autonomy from the ground. In normal circumstances, we assume the data are downloaded to ground once every four station passes [RD 4].

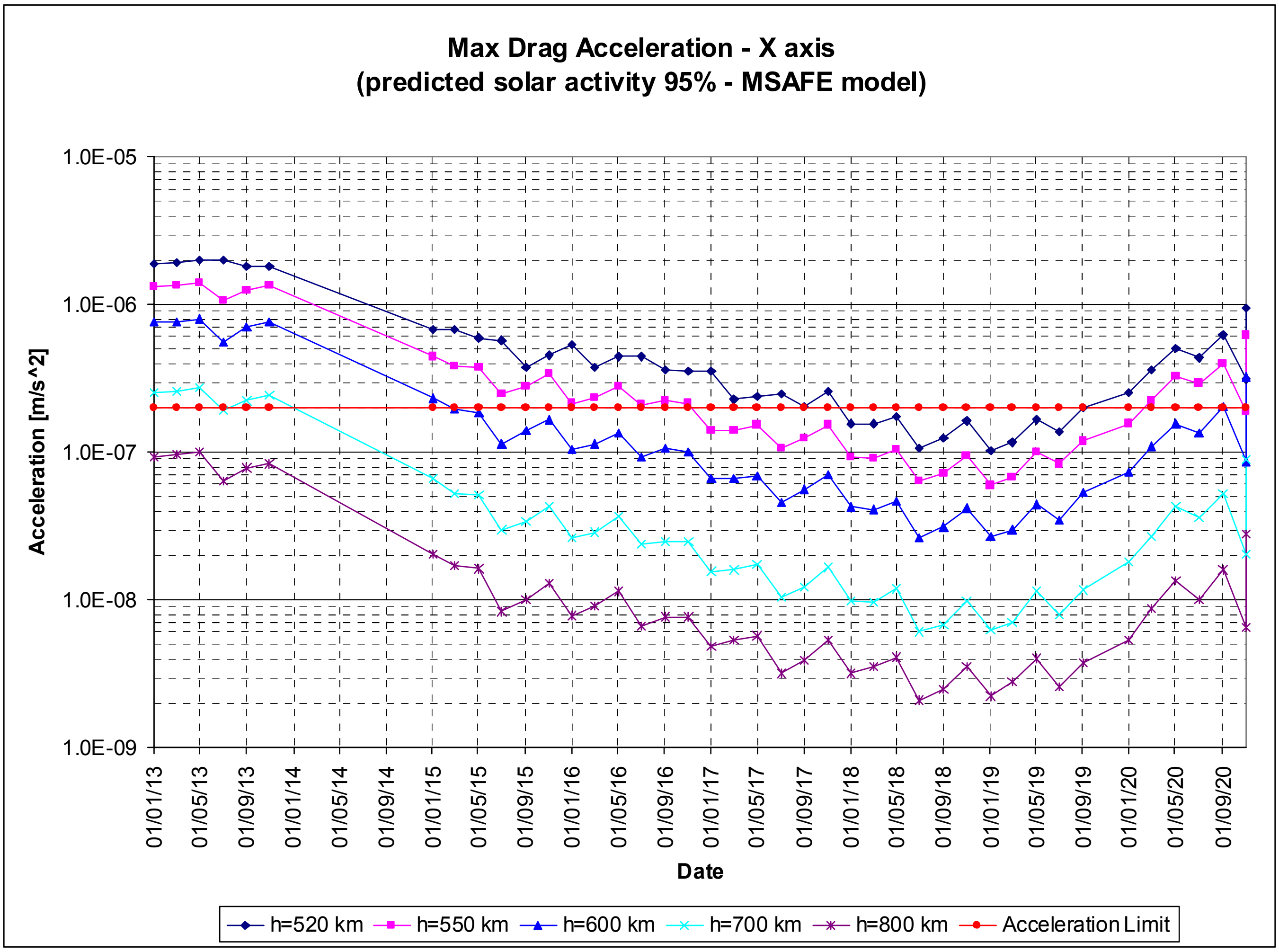

Figure 2.2-1: Parametric analysis of the drag acceleration.

A mission launched after 2012 will take place in the descending leg of solar cycle 24, moving toward the next solar minimum around 2019. The downward trend of the solar flux is reflected in similar trend of the mean atmospheric density at a given altitude. The drag acceleration shown in this plot is calculated by means of the MSIS density model from the solar flux forecast at the 95% probability level published by NASA in June 2008. The area-to-mass ratio is 0.0046 m^2/kg. A notable innovation, introduced in this study, is to specify the GG mission in terms of a maximum acceleration level, rather than a fixed launch altitude. This allows the experiment and drag free design to be carried out and frozen, independent of the launch date. The launch altitude will be adjusted once the launch epoch is known, in order that the maximum design acceleration is not exceeded. The launch altitude will vary anyway between boundaries, 500 km to 700 km, which affect neither the launcher capability, nor the experiment signal magnitude.

The selected maximum drag acceleration level is 2.0E-7 m/s^2. A drag acceleration level < 2.0E-7 m/s^2 requires a launch altitude of 700 km from October 2014 on. From October 2015, the launch altitude can be reduced to 600 km.

4. SPACECRAFT DESIGN

4.1 Mechanical and Thermal Design

The main drivers of the satellite mechanical configuration are:

- compatibility with Vega launch vehicle and reference fairing envelope;
- outside shape with cylindrical symmetry;
- easy integration of PGB
- low area-to-mass ratio (< 0.005 m²/kg)
- spin axis must be a principal axis of inertia
- $J_{SPIN} > J_{TRANS}$
- $\beta = (J_{SPIN} - J_{TRANS})/J_{TRANS} \cong 0.2 - 0.3$.

The driving thermal control requirements of GG include:

- test mass mean temperature stability better than 0.1°C/day;
- Axial temperature gradient at the level of the proof masses shall not exceed 1°C/arm length (previous value < 4°C/m);
- Temperature fluctuations in the proof masses shall not exceed 0.2 °C in 1 day;
- Linear temperature drift in the proof masses shall not exceed 0.2°C/day;
- Electronic units (assumed): -20/+50°C operating temperature; -30/+60 °C non operating temperature.

The requirements of GG do not allow reuse of a standard platform. The proposed solution is an ad-hoc structure with high cylindrical symmetry, supporting the PGB and equipment.

The spacecraft body is about 1.5 m wide and 1.5m high. The experimental apparatus is accommodated in a nested arrangement inside the body. The structure is made up of a central cylinder and an upper and lower truncated cone. The upper cone is removable to allow the integration of the PGB with its suspension springs; the lower cone supports the launcher interface ring. Sensors and electric thrusters are mounted to the central belt. Two S-band antennas, both fixed, are aligned with the spin axis.

The solar array is made of two cylinders separated by a central belt for mounting equipment, including thrusters and sensors; this solution also allows a suitable distribution of thermal covers and radiators to realize an efficient thermal control.

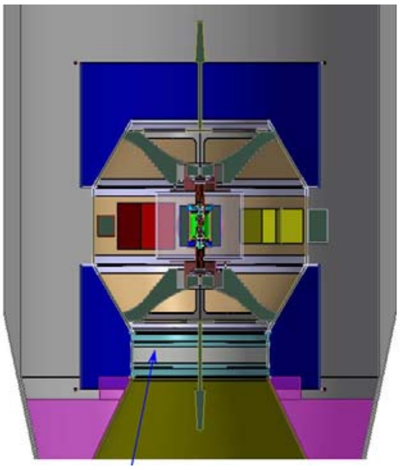

Launch configuration with supplementary launch adapter

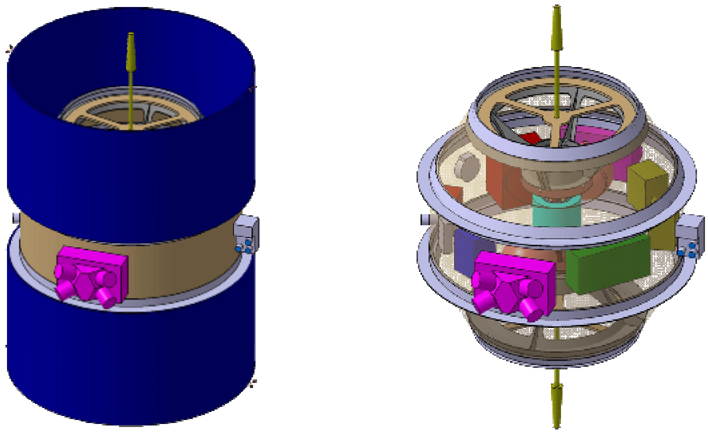

Flight configuration (left) Same with solar panels removed and equipment layout shown (right)

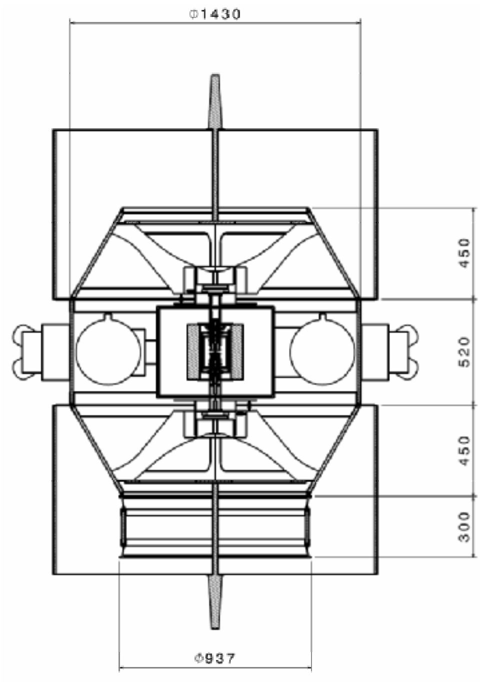

Main dimensions

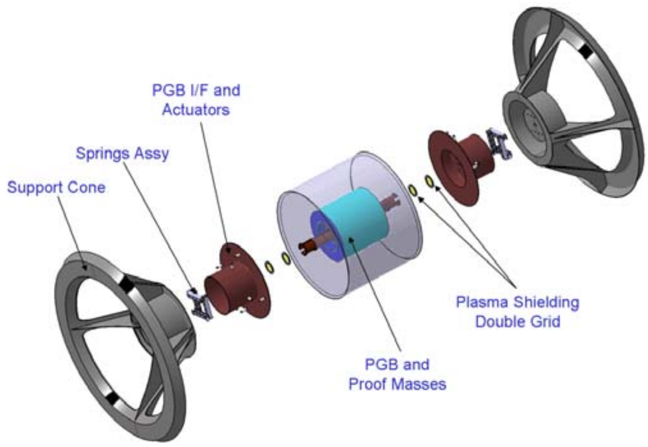

PGB mechanical interface

Figure 4.1-1 : GG satellite configuration.

The current implementation of the above-described configuration concept has evolved in this Phase A2 study, as follows.

- To reduce cost, implementation of standard (current-generation) pieces of equipment from the PRIMA platform set was imposed (e.g., transponders, CDMU). These boxes are generally larger than would be possible in an optimized GG-dedicated design. In addition, to avoid costly redesign, all boxes were placed inside the spacecraft body, allowing simpler thermal control. As a consequence, the volume of the spacecraft inflated considerably w.r.t. the previous design exercises. This is not considered critical since VEGA allows volume and mass increase well beyond any such requirements of GG.
- The implementation of the FEEP based Microthruster solution benefited considerably from the design data of the current FEEP implementations in Microscope and LISA Pathfinder. A realistic power demand estimate was provided by ALTA, which, together with a detailed design of the solar array, also based on up-to-date parameters, led to an increased area being required for the solar panels. This was accommodated by suitably sizing the panels, while maintaining compliance with the inertia and area-to-mass ratio requirements. This configuration however does not allow further growth (without affecting the inertia and area ratios) and a strict power budget limit must be imposed.
- To make room for the lower solar panel, while remaining compatible with the standard Vega 937 B adapter used for launcher separation, another structural adapter piece had to be introduced.
- A dedicated spacecraft-to-experiment mechanical interface structure was devised.

Layout optimization was performed and inertia and mass balancing was verified compliant with the requirements. A realistic envelope of the FEEP thruster clusters was implemented. Definition of the interface details of such payload elements as capacitance plates, inch-worms and launch-lock mechanisms was much improved.

Very detailed structural and thermal models were implemented and the corresponding analyses were performed [RD 13] [RD 14]. Compliance with the requirements was proven and mass and power resource requirements were updated to reflect these findings.

4.2 Functional and Electrical Design

The GG electrical architecture is shown in the block diagram of Figure 4.2-1.

The on-board data handling system will be based on one CDMU, derived from the standard LEONARDO unit, developed via the ASI PRIMA program and based on an ERC32 CPU. The CDMU delivers commands and exchanges data with two payload electronics units, the PGB Control and Processing Electronics (CPE), located on the spacecraft platform, and the Experiment Control Electronics (ECE), housed inside the PGB.

The CDMU includes a Mass Memory devoted to science and HK data storage. The housekeeping data rate is estimated to be about 10 kbps. The science data rate, including payload housekeeping, is 12.7 kbps (see Table 4.3-3). The total data rate including 20% packet overhead is 27.2 kbps. The total amount of data produced in 1 orbit is 155 Mbit. An on board mass memory sized for 24-hour autonomy amounts to about 2.4 Gbit.

An S-Band architecture derived from the PRIMA platform is proposed for the GG TT&C, with minor modifications implemented in the RF distribution network because of the different mission scenario and attitude. The component elements include:

- 2 transponders with low output power (23 dBm, i.e., 200 mW) and diplexer embedded;
- RFDN miscellanea in coaxial technology (2 RF switches and connection cables)
- 2 LGAs with circular polarization (LHCP or RHCP) and hemispherical coverage (gain = -3 dBi at ±95° boresight offset angle).

The Assuming Rice-algorithm data compression (compression factor = 2.8), four station contacts per day, of 10 minute duration, are enough to download the whole mass memory content at a telemetry rate of 350 kbit/s.

The Electrical Power System is required to provide around 500W for both payload and S/C equipment, constantly along the whole mission duration. The EPS is implemented by a dedicated Power Distribution and Control Unit (PCDU), plus a solar array and a battery.

The solar array consists of two identical cylindrical Al honeycomb panels with CFRP skins, covered with 3G GaAs/Ge Triple Junction solar cells with 28% efficiency. Cells are stacked vertically on the cylinder surface to form strings. The length of a single cell determines how many such stripes can be disposed while the height limits the number of cells per string. The specific power at BOL at 30-deg sun incidence is about 420 W/m^2. The array can sustain the load power demand of 510 W during the sunlit period, including a power request of 180 W for recharging the battery, and assuming 95% BCR efficiency. The calculated system margin after 2 years is about 10%, limited by the size constraints of the array (driven by experiment requirements such as area-to-mass ratio and inertia ratio).

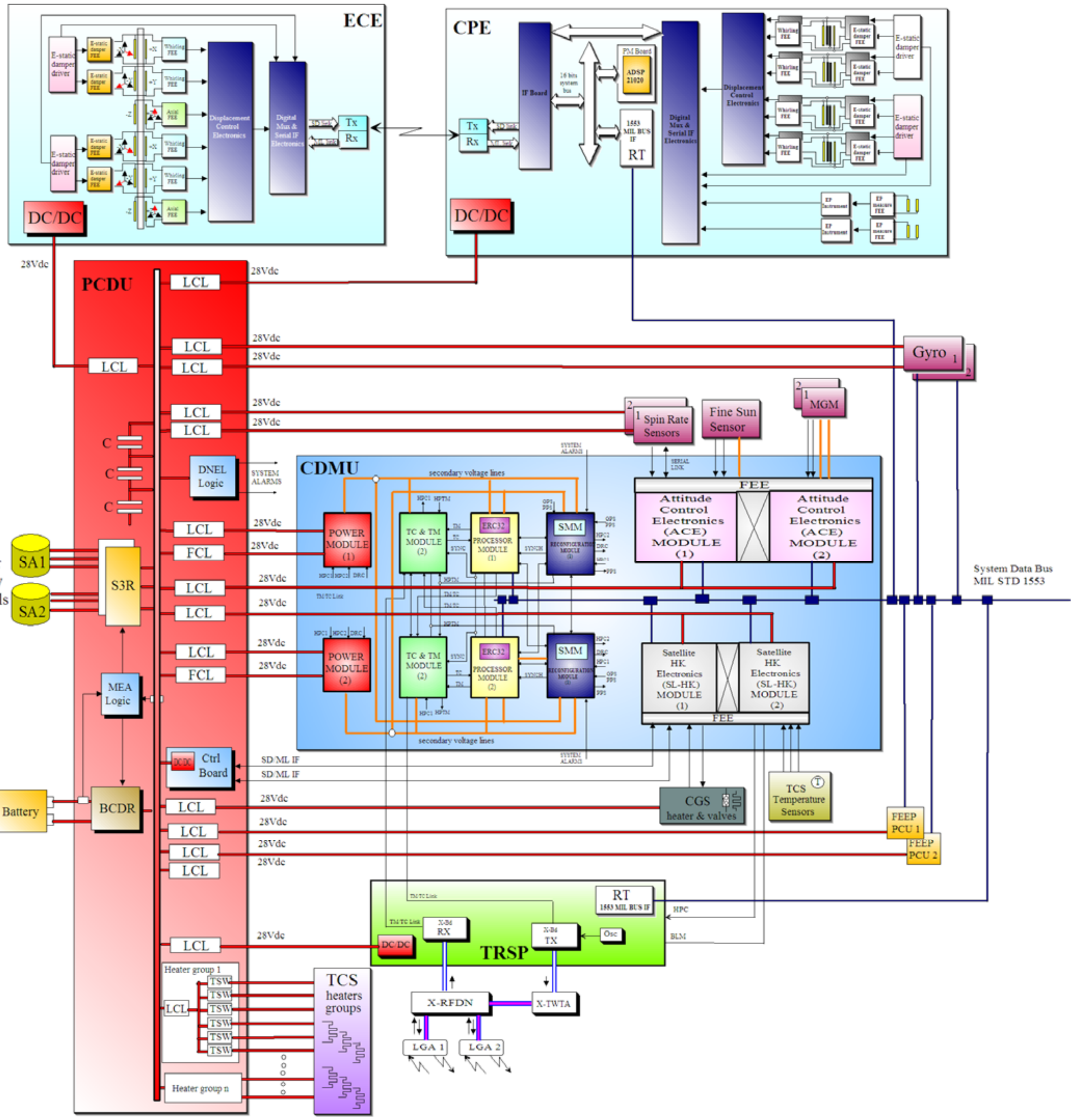

Figure 4.2-1: GG electrical architecture.

4.3 Resources and Budgets

The tables attached provide the status of the resource budgets after the Phase A2 study.

The satellite separated dry mass budget amounts to about 428 kg including 20% system margin. The propellant mass is less than 10 kg in the FEEP micropropulsion option. A two-stage launcher adapter is needed to reach the Vega interface allowing a sufficiently tall solar array. The total launch mass including adapters and all margins is about 518 kg.

The power demand of the satellite is about 500W. This is a large increase w.r.t. the previous studies, motivated by a 3-fold increase of the estimated FEEP power demand.

The data generation rate, shown in Table 4.3-3, is compatible with large margins with the limit telemetry rate of the chosen S-band system and ground station.

Table 4.3-1 : Satellite mass budget.

Galileo Galilei					
	Target Spacecraft Mass at Launch			1000,00	kg
	Below Mass Target by:			482,18	kg
	Without Margin	Margin		Total	% of Total
Dry mass contributions		%	kg	kg	
Structure	**104,61 kg**	**18,09**	18,92	**123,53**	23,86
Thermal Control	**8,70 kg**	**20,00**	1,74	**10,44**	2,02
Communications	**9,60 kg**	**10,00**	0,96	**10,56**	2,04
Data Handling	**16,00 kg**	**20,00**	3,20	**19,20**	3,71
AOCS	**5,92 kg**	**13,11**	0,78	**6,69**	1,29
Propulsion	**37,66 kg**	**13,95**	5,26	**42,92**	8,29
Power	**57,68 kg**	**14,82**	8,55	**66,23**	12,79
Harness	**12,50 kg**	**20,00**	2,50	**15,00**	2,90
Payload	**55,34 kg**	**12,77**	7,07	**62,41**	12,05
Total Dry(excl.adapter)	**308,01**			**356,98 kg**	
System margin (excl.adapter)		**20,00 %**		**71,40 kg**	
Total Dry with margin (excl.adapter)				**428,38 kg**	
Other contributions					
Wet mass contributions					
Propellant	**4,75 kg**	**100,00**	4,75	**9,50**	1,83
Adapters mass (including sep. mech.), kg	**79,94 kg**	**0,00**	0,00	**79,94**	15,44
Total wet mass (excl.adapter)				**437,88 kg**	
Launch mass (including adapter)				**517,82 kg**	

Table 4.3-2 : Satellite power budget.

Power Budget (Configuration with 2 FEEP clusters)					Sunlit	Eclipse	
Equipments	No. Of active	Unit Power [W]	Contingency [%]	Power with Contingency [W]	Nominal Power [W]	Nominal Power [W]	LEOP phase [W]
ECE	1	9	20	10.8	10.8	0	0
CPE	1	18	20	21.6	21.6	0	0
Total P/L [W]					**32.4**	**0.0**	**0.0**
CDMU	1	18.0	10	19.8	19.8	19.8	19.8
TRSP1 (Tx + Rx)	1	20.0	3	20.6	20.6	20.6	20.6
TRSP 2 (Tx + Rx)	1	6.5	5	6.8	6.8	6.8	6.8
PCDU	1	25.0	10	27.5	44.5	27.5	27.5
Battery (max charging)	-	-	-	-	180.0	0.0	0.0
TCS (heaters)	1	12.0	20	14.4	14.4	30.0	30.0
Fine Sun sensor	1	1.3	10	1.4	1.4	1.4	0.0
Gyro	0	19.8	10	21.8	0.0	0.0	21.8
Rate Sensor	1	6.0	10	6.6	6.6	6.6	0.0
Magnetometer	3	0.8	10	0.9	2.6	2.6	2.6
FEEP (2 cluster option)	1	133.0	20	159.6	159.6	159.6	0.0
Total Service Module [W]					**456.4**	**275.0**	**129.1**
Total Satellite [W]					**488.8**	**275.0**	**129.1**
PCDU loss [2%]					9.8	5.5	2.6
Harness loss [2%]					10.0	5.6	2.6
GRAND TOTAL w/o system margin [W]					**508.5**	**286.1**	**166.5**

Table 4.3-3 : Satellite data budget.

Data description	Variable list	Number of variables	Freq. [Hz]	Record length [bit]	Data rate [kbit/s]
Diff. TMs displacement	0x, 0y	2	50	16	1.6
Tme/PGB displacement	0x, 0y, 0z	3	50	16	2.4
Tmi/PGB displacement	0x, 0y, 0z	3	50	16	2.4
PGB/Spacecraft displac.	0x, 0y, 0z	3	50	16	2.4
0_{SPIN}	0_x, 0_y, 0_z	3	50	16	2.4
Reference time	t	1	50	16	0.8
Science data					**12.0**
PGB whirl monitoring	Sensing + actuation	6	1	16	0.096
Tme whirl monitoring	Sensing + actuation	6	1	16	0.096
Tmi whirl monitoring	Sensing + actuation	6	1	16	0.096
ADC monitoring	Number of ADC	9	1	16	0.144
Inchworm monitoring	Number of inchworms	6	1	16	0.096
Piezo monitoring	Number of piezo	6	1	16	0.096
PGB Inner temperature monitoring	Number of temperature sensors	20	0.10	16	0.03
Capacitance bridge monitoring	Number of capacitance bridges	9	0.10	16	0.01
Payload HK					**0.7**
Commands to FEEP	Number of commands	6	1	16	0.096
PGB/Spacecraft phase lag	Number of lag sensors	1	0.10	16	0.0016
Commands to actuators	Number of commands	6	50	16	4.8
Sun sensor	1 (2 in case o redundancy)	2	50	16	1.6
FEEP monitoring	Number of FEEP	6	1	16	0.096
DFACS					**6.6**
			Total Data Rate	kbps	**19.3**
			Altitude	km	**520**
			Period	s	**5702**
			Data volume	Mbit/orbit	**110**
				Mbit/day	**1664**

5. GROUND SEGMENT CONCEPT

The preliminary mission and operations requirements of the GG satellite can be summarized as follows [RD 23]:

- Equatorial orbit at altitude around 600 km
- Utilization of the ASI/Malindi Ground Station. Additional ground station support to be considered only during early orbit phase and critical spin-up maneuver
- Four daily communication passes for TM reception and TC uplink
- Single experiment mission running continuously up to the end of the nominal mission (1 year)
- No scientific quick look required, all science data processing made off-line as bulk data
- No maneuvers, orbital changes or attitude slews during the scientific mission
- Autonomous scientific operations, executed as time tagged sequences loaded at least one day in advance.

The nominal ground station for mission operations is the ASI GS in Malindi. Additional ground stations may be considered to support the LEOP (for example the ESA Kourou Station that also satisfies the equatorial requirements).

The Ground Communication Network connects the Ground Stations with the Operations Control Centre (OCC), and the OCC with the Science Operations Centre (SOC). This network will be realized using the existing multi-mission ASINET Operational Network.

The Operations Control Centre (OCC) is responsible for the overall execution of the GG mission operations, in terms of mission planning, spacecraft monitoring and control, orbit and attitude determination, payload monitoring and control. The OCC will route the scientific telemetry to the SOC and will receive the P/L command requests from the SOC to be subsequently processed and uplinked to the satellite. In the current concept, ASI will provide the OCC in the LEOP phase, whereas the scientific mission will be under the control of a dedicated control room at ALTEC.

The Science Operations Centre (SOC) is normally responsible for the scientific data processing and analysis, and for generating the scientific operation sequences to be executed on board. GG is a PI-type mission, where all the data will remain in the possession of the PI, at the University of Pisa, until the first science products have been generated, after which the data will be moved into the public domain. For the GG mission, no real-time involvement of the SOC in the mission operations is required, and the operation sequences are changed very infrequently, if at all, once the experiment has been set up. Therefore, a simple Internet link is envisaged for exchanging the science data between OCC and SOC in an “off-line” mode.

CONTROLLED DISTRIBUTION

6. CRITICAL TECHNOLOGIES AND SPECIFIC ISSUES OF THE GG MISSION

6.1 Drag Free and Attitude Control System

After launcher separation, the Drag-Free and Attitude Control System (DFACS) provides spacecraft attitude control, and spacecraft spin-up to the required spin rate of 1 Hz. Thereafter, the PGB is unlocked and the microthrusters are enabled. From then on, the DFACS provides drag compensation with very high rejection ratio, as well as whirl control and control of the spacecraft spin rate and of the PGB-spacecraft relative rotation rate, necessary for maintaining the integrity of the PGB suspensions.

The early attitude modes use sun sensors and magnetometer for attitude determination, supplemented with a gyroscope in eclipse and for FDIR, and impulsive cold-gas thrusters as actuators. In the science measurement phase, four independent controllers are active (Figure 6.1-1):

- The *XY drag-free controller*, for drag compensation in the XY plane. This controller shall reduce the drag disturbances at the spin rate providing a rejection better than 2 10^{-5};
- The *XY whirl controller*, for stabilizing the motion in the XY plane, by a low-frequency action;
- The *Z drag-free controller*, for drag compensation and displacement reduction along the Z axis;
- The *Spin-axis angular rate controller*, to limit the relative rotation between PGB and satellite.

The XY drag free controller uses the microthrusters for actuators, in closed loop with the capacitance sensors of the science accelerometers (in common mode). The control of the Z displacement and of the whirl is realized by acting on the capacitance plates. Supplementary sensors include the spin rate sensor, for accurate determination of the fractional spin rate change, and photo-detectors for the phase lag between the PGB and the spacecraft outer shell. The latter control action is actuated by the microthrusters.

The XY drag-free controller is the most challenging task, considering the very fine drag compensation required and the limitation on the response time of the available actuators, which reduces the usable command update rate.

The DFACS requirements, architecture, algorithms, the specific technologies and the analysis results are documented in [RD 16]. The design of the basic algorithms for fine drag compensation is done; during Phase B, it will be completed with additional logics not relevant to the performance but to system robustness (failure detection and isolation, sensor monitoring, etc.).

The results from the analysis and simulation show that the proposed solutions meet the requirements with adequate margins, with the available technologies (Figure 6.1-2). Few remaining non compliances on the thrusters performance (Table 6.2-1), particularly as regards response time and maximum centrifugal acceleration, are considered minor.

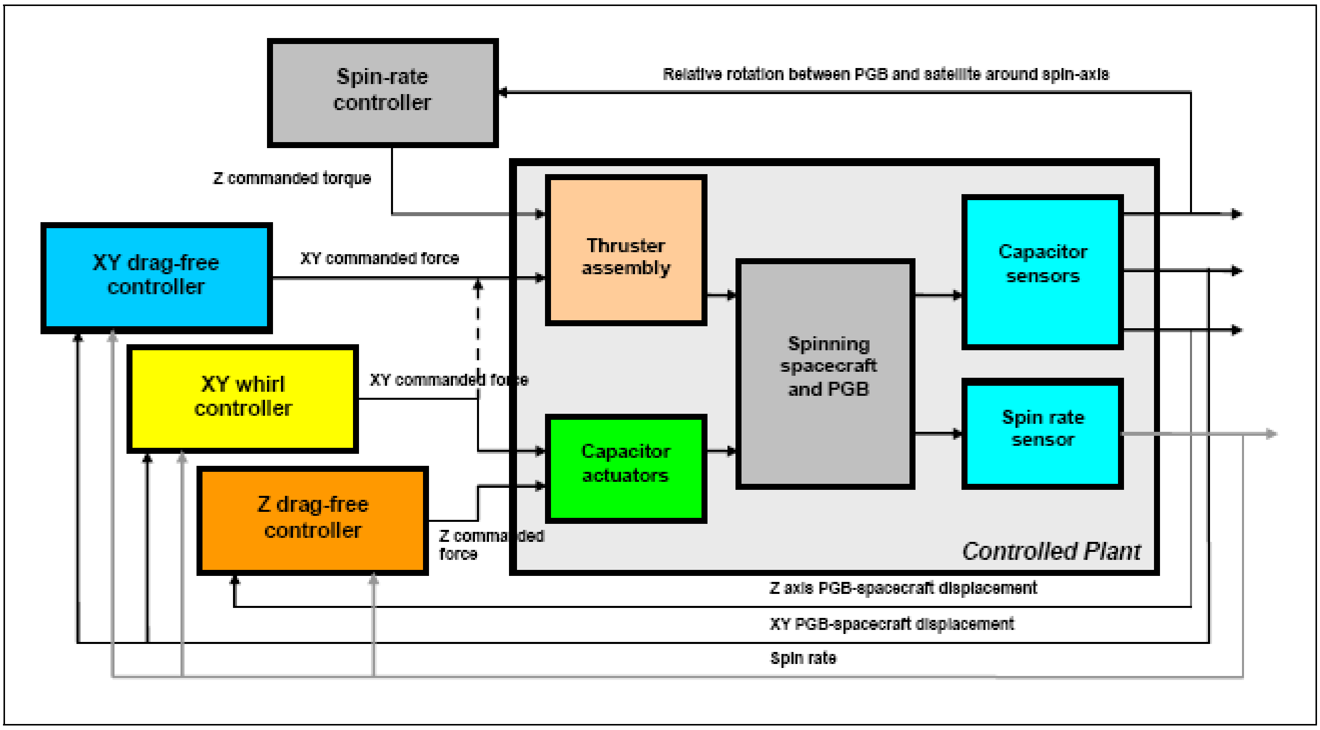

Figure 6.1-1: Linear axis control architecture.

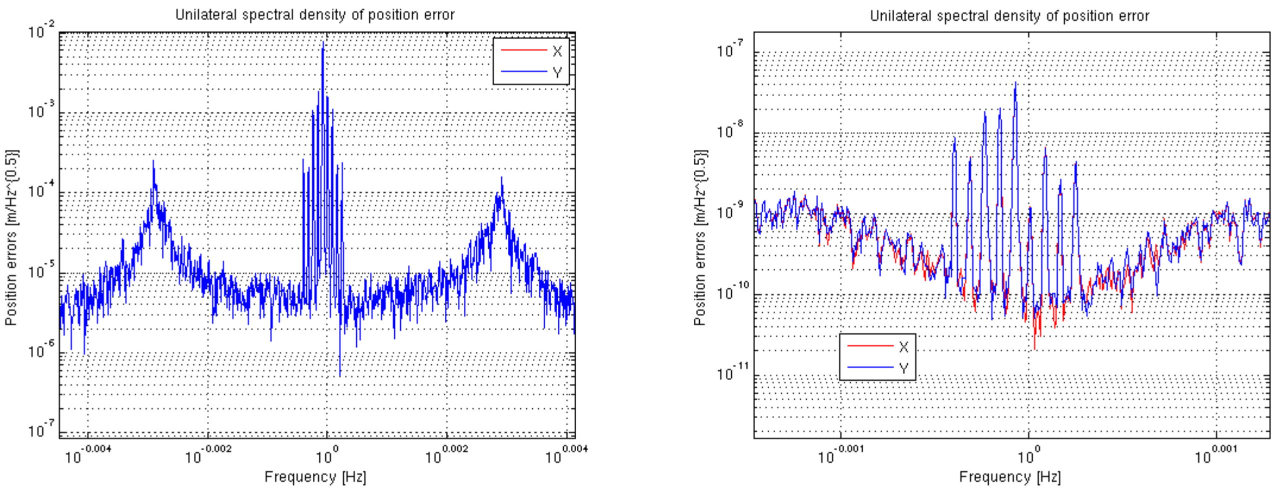

With whirl control, without drag control   With whirl and drag control

Figure 6.1-2: Drag control performance.

Zoom around 1Hz of the one-side spectral density of the PGB-spacecraft COMs relative position. Body reference frame; relative uncertainty on angular rate knowledge equal to 10^{-4}. By comparing the maxima of the spectral density around 1Hz on the left (no drag control) and on the right (with drag control), one can observe that the drag disturbance rejection provided by the XY drag-free controller is better than 1/150,000 even with worst case uncertainty on angular rate knowledge.

6.2 Micro-Newton Thrusters

The drag-free and attitude control microthrusters must produce finely tuned (in magnitude and frequency) forces, using tiny amounts of propellant in order to minimize perturbations on the test bodies from nearby moving mass. Micro-Newton thrusters are fundamental to achieving the objectives of the EP experiment, and a design driver of the spacecraft configuration. In the past, lack of demonstration of the performance of such microthrusters weighed heavily in the assessment of maturity of all missions proposing to test the EP in space. Considerable progress was made in recent years, and qualification of microthrusters for such programs as GAIA, Microscope and Lisa Pathfinder is nearing completion.

The solution envisaged in the past GG studies was based on Field Emission Electric Propulsion mini-thrusters. These thrusters are very attractive because of the high specific impulse (gas velocity at nozzle exit > 6 km/s) and consequently low propellant mass (a few grams of Cesium suffice for 2 years). Conversely, FEEP has high power to thrust ratio even when compared with other electric propulsion system. The required thrust is in the same range as needed for the FEEP thrusters under development for the Microscope and Lisa-Pathfinder missions.

Thruster requirements were derived as part of the DFACS tasks (Table 6.2-1). A review of the status of the FEEP thrusters was performed with the collaboration of ALTA [RD 19]. Assessment of an alternative option based on the GAIA cold-gas microthrusters, produced by TAS-I, was performed too [RD 20]. The comparative analysis [RD 16], performed on the basis of a detailed list of performance and design requirements, found that both thruster types are in principle suitable and mature for GG, although some areas require further investigation. The FEEP implementation was taken as the design reference for this study; however, a final decision is deferred until Phase B, when the outcome of the ongoing microthruster qualification efforts will become available.

Table 6.2-1: Thruster requirements (Spin rate: 1Hz).

No	Parameter	Unit	Value	Comments
1	Maximum thrust	µN	>=150	50% margin
2	Max thruster response time[1]	ms	40	@ commanded step (up and down) >= 60 µN
3	Resolution (quantization)	µN	24	TBC, not critical
4	Max noise	µN/√Hz	18	Around 1Hz
5	Scale factor error	%	12	Peak
6	Update com rate	Hz	10	TBC
7	Total impulse	Ns	4500	20 % margin
8	Minimum thrust	µN	<=10	TBC
9	Vector stability	rad	0.17	Peak, at 60 µN
10	Centrifugal acceleration	g	<4.4	20 % margin, 0.75m spacecraft radius

[1] Thrust response time is defined as the time required to achieve the 90% of the commanded step, and to remain indefinitely above this threshold.

6.3 Spin Rate Sensor

Accurate angular rate measurement by standard sensors (star trackers, sun sensors, earth sensors) becomes critical at large spin rate. Star trackers cannot measure the position of objects moving faster than few tens of deg/s, while sun/earth sensors are not very accurate. In the previous phases of GG studies, this fact was highlighted as one of the critical aspects of the project. This motivated a dedicated breadboard development undertaken as part of this study [RD 21].

The proposed solution for the accurate rate sensor consists of a camera using a Position Sensing Detector (PSD) for measuring the optical power and the coordinates of the light spot focused on the focal plane. A PSD is a four-electrode photodiode in which the photocurrent generated in a given point by a light spot shares between the electrodes proportionally to the position of the spot on the PSD plane. PSD are fast sensors (typical response time = 350 ns) and can provide very accurate position measurement of the light spot (at the nm level, provided sufficient signal/noise ratio is built up), which translates into an accurate angular measurement via the camera focal length. A small telescope endowed with the sensor detects position of light emitting source from the position of the light spot focused on the PSD.

A prototype of this novel rate sensor was designed, a performance model was prepared, and the breadboard was manufactured and successfully tested within this Phase A2 (Figure 6.3-1).

From left to right: (top) spacers and retaining rings; (bottom) detector box, sensor body, internal optics barrel

Fully integrated spin rate sensor

Fully integrated spin rate sensor

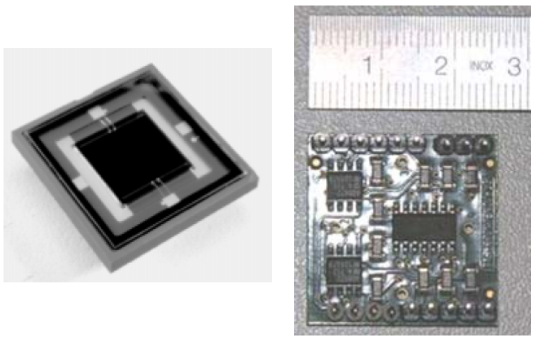

PSD and front-end electronics

Figure 6.3-1: Parts of the spin sensor breadboard.

6.4 Software Simulators

A numerical Space Experiment Simulator is a crucial for all space experiments that rely in a fundamental way on zero-g, and therefore cannot be tested on the ground at any level close to the required science performance.

The GG Space Experiment Simulator was initiated, with ASI support, since the first study of the mission. This preliminary simulator allowed the basic physical features of the GG system to be identified and checked; however, it was mostly a 2-dimensional model. Building up on the expertise acquired with the GOCE Simulator, the GG Space Experiment Simulator has now been raised to a very advanced level in the very short time span of the Phase A2 study. By incorporating in it the physical parameters as experimentally measured in the lab with the Payload Prototype, the accuracy of the simulation was correspondingly enhanced. The combination of (a) flight validation of the orbit and spacecraft environment simulation and (b) lab validation of the experiment parameters makes the GG simulator an extremely reliable performance validation tool, the like of which was seen in no other similar mission.

Throughout the Phase A2 study, the following steps were performed.

- The latest version of the simulator, inherited from the previous studies, was reviewed and updated in order to reflect the current experiment design concept. The simulator architecture is fully modular, which makes it easy to maintain a working version by plugging in the updated modules as they become available.
- This initial GG system simulator included a model of the spinning satellite constituted by six rigid bodies (spacecraft, PGB, two proof masses and two mechanical suspensions - flat gimbals - connecting the PGB to the test masses). The bodies are connected according to the topology of the true system. A validation campaign on a new hardware platform was carried out.
- A preliminary set of planar (XY plane) simulations was initially carried out to refine the model and verify the performance of the Whirl Control (2-body problem, 6-body problem, with the assumption of no external drag or residual drag).
- Then, a full 3D model of the 6-body system was realized (Figure 6.4-1), providing 6 degrees of freedom to spacecraft, PGB and proof masses and 2 rotational degrees of freedom to the gimbaled arm of the suspension (the gimbals allow conical-only movements of the coupling arm of the suspension). The validation was successful.
- The drag-free control law and the model of the actuators adopted for the drag free compensation were updated according to the latest design.
- Updating of the models of the disturbing forces which can mask/mimic the EP violation signal, and the noise affecting the experiment, was performed
- A model of the EP violation signal was implemented in the simulator.

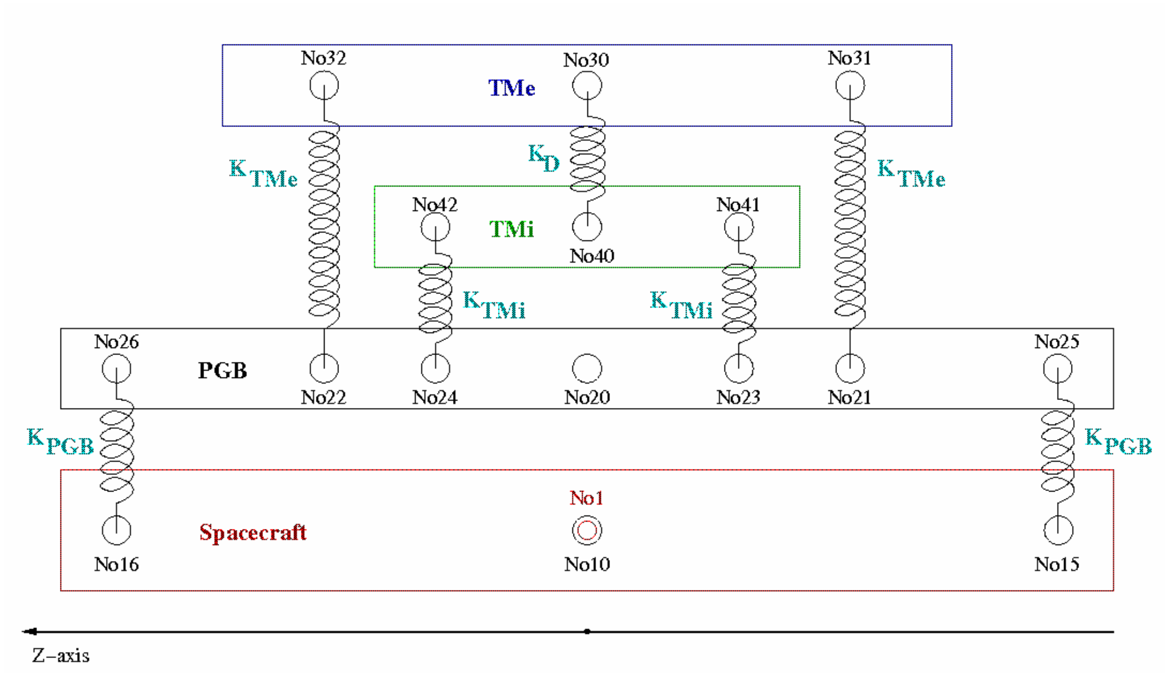

Figure 6.4-1: Schematic model of the GG dynamics system.

Logical scheme of the dynamical model implemented in the DCAP software environment for finite element simulation of the space experiment. The z axis is the spin/symmetry axis of the system; all elastic connections along z are very stiff; the plane of sensitivity is perpendicular to z. The model encompasses all bodies (spacecraft, PGB and 2 test masses), each one with its 6 degrees of freedom in 3D (3 for translation and 3 for rotation), mass and moments of inertia. All non rigid components of the system (sketched as springs) are implemented with their design stiffness (in the sensitive plane as well as in the z direction) and mechanical quality factors.

At the end of the above-listed steps, the simulator was ready for its task, i.e., analysis and trade-off of the science performance vs. Drag Free Control and Whirl Control capabilities. The simulator will produce good indications of the ultimate limit of the science performance depending on the imperfections and noise allocated for the sensors and actuators.

The simulator is capable of excluding one or more control loops (e.g. the Test Mass whirl control, or DFC) from the system in order to analyze and exploit the limit performance for each simplified scenario. This permits to identify each critical point and to establish a hierarchical list of priorities vs. science performance (e.g. the absence of the DFC puts a certain requirements on the Common Mode Rejection Ratio of the mechanical suspension in order to reach a given science performance).

In addition, the introduction of the EP violation signal in the simulator provides the capability to test the post processing algorithms that will provide the measurement of the Eötvös parameter.

The documentation of the simulator architecture and the results of the science performance simulation are in [RD 18]. The simulator was also used for the prediction of the ultimate performance of the experiment, documented in [RD 7] and summarized in Table 6.4-1.

Table 6.4-1: GG Experiment Error Budget

The amplitude of the error at the orbit frequency is smaller than the signal by a factor about 4. The largest systematic error is at twice the orbit frequency, with an amplitude one order of magnitude larger than the signal. This error can be easily distinguished from the signal during data processing, since the duration of each elementary experiment is about one week. The error at the whirl frequency is removed during the synchronous demodulation of the post-processing.

Acceleration (transverse plane) due to:	Frequency in IRF (Hz)	Frequency in BF (Hz)	Phase	Differential acceleration (m/s²)	Differential displacement (pm)
EP signal	ν_{orb}	ν_S (wrt Earth)	X_{LVLH}	$8.377\cdot10^{-17}$	0.62
External non gravitational forces	ν_{orb}	ν_S	Mainly along Y_{LVLH}	$2\cdot10^{-7}$	-
External non gravitational forces after DFC compensation and CMRR	ν_{orb}	ν_S	Mainly along Y_{LVLH}	$4\cdot10^{-17}$	0.29
Earth coupling with TMs quadrupole moments	ν_{orb}	ν_S	X_{LVLH}	$1\cdot10^{-17}$	0.07
Radiometric effect along Z coupled with Earth tide	$2\cdot\nu_{orb}$	$\nu_S \pm \nu_{orb}$	X_{LVLH}	$1.4\cdot10^{-15}$	10.7
Emitted radiation along Z coupled to Earth tide	$2\cdot\nu_{orb}$	$\nu_S \pm \nu_{orb}$	X_{LVLH}	$4\cdot10^{-17}$	0.29
Tide coupled to non grav. acceleration along Z	$2\cdot\nu_{orb}$	$\nu_S \pm \nu_{orb}$	X_{LVLH}	$3\cdot10^{-17}$	0.23
TM1 inner magnetic dipole coupled to $B_\oplus$ magnetized TM2	$2\cdot\nu_{orb}$	$\nu_S \pm \nu_{orb}$	X_{LVLH}	$1\cdot10^{-18}$	$9\cdot10^{-3}$
TMs inner magnetic dipoles coupled to $B_\oplus$	$2\cdot\nu_{orb}$	$\nu_S \pm \nu_{orb}$	X_{LVLH}	$6\cdot10^{-21}$	$5\cdot10^{-5}$
TM1 and TM2 with $B_\oplus$ induced magnetization couple	$4\cdot\nu_{orb}$	$\nu_S \pm 3\cdot\nu_{orb}$	X_{LVLH}	$8\cdot10^{-23}$	$6\cdot10^{-7}$
TM1 with $B_\oplus$ induced magnetization couples with $B_\oplus$	$4\cdot\nu_{orb}$	$\nu_S \pm 3\cdot\nu_{orb}$	X_{LVLH}	$8\cdot10^{-24}$	$6\cdot10^{-8}$
Whirl motion coupled to Earth tide	ν_w, $\nu_w \pm 2\cdot\nu_{orb}$	$\approx\nu_S \pm \nu_w$ ($\nu_{orb} << \nu_w$)	X_{LVLH}	$7.3\cdot10^{-14}$	538
…	Higher frequencies	Frequencies far from ν_S	X_{LVLH}	…	…

7. DEVELOPMENT APPROACH AND PROGRAMMATICS

The objectives of the GG program are:

- To carry out a test of the Equivalence Principle with sensitivity of a least 1 part in 10^{17}, in low, near-equatorial, near-circular Earth orbit, for a duration of at least 1 year;
- To design, develop, and test a small satellite, devoted to the above objectives, over a time span (Implementation Phase) not exceeding 3 years (TBC), within a level of resources commensurate with that of a small satellite program of ASI;
- To launch and operate the satellite using as much as possible the infrastructure and resources of ASI;
- To use this opportunity to advance the implementation and use of Italian technology and know-how in the service of an outstanding scientific project.

A number of elements support the project during its life cycle. Most notably:

- The GG Payload ground prototype (GGG) is an experiment to test the Equivalence Principle, at lower sensitivity, with an apparatus very close to a prototype of the payload designed for the GG space experiment. The experiment is carried out at the University Of Pisa and will be used as a development model for the flight model.
- The End-to-End Simulator, described in §6.4, will be used during the project lifecycle to consolidate the design, verify requirements in advance respect to the HW manufacturing, execute tests not performable on real HW.

For the satellite development, a Proto Flight approach is proposed. Prior to the PFM program, the satellite functional performances will be validated using the dedicated End to End simulator and an Avionics Test Bench where representative hardware will be incrementally included in the loop. Since one complete satellite model is planned, it will be subjected to a complete proto-flight test campaign in order to confirm the functional validation performed on simulators, and the thermo-structural performances evaluated by analysis (

Figure 6.4-2).

At payload level, the PFM approach is complemented by a PGB-STM (Structural Thermal Model), used to qualify the mechanical and thermal design, including the thermo-structural deformation aspects. The PBG-PFM will be used to complete the acceptance from the mechanical, thermal and functional point of view, and will be the flight unit.

At equipment and subsystem levels, the verification approach will be defined as function of the individual unit/subsystem Technology Readiness Level (TRL). The general approach is to have a complete qualification test campaign and consequently a qualification approach on the new items, and to perform a reduced acceptance campaign on the recurring units. The former include the microthrusters, the spin sensor, the ECE and the experiment launch lock mechanisms, for which development and/or qualification models are planned.

The GG program is phased according to the following durations and reviews (Figure 6.4-1):

- Phase B: 9 months, ending with the PDR
- Phase C/D: 36 months, with an intermediate CDR milestone, ending with the FAR

- Phase E: 3 months, ending with LRR.

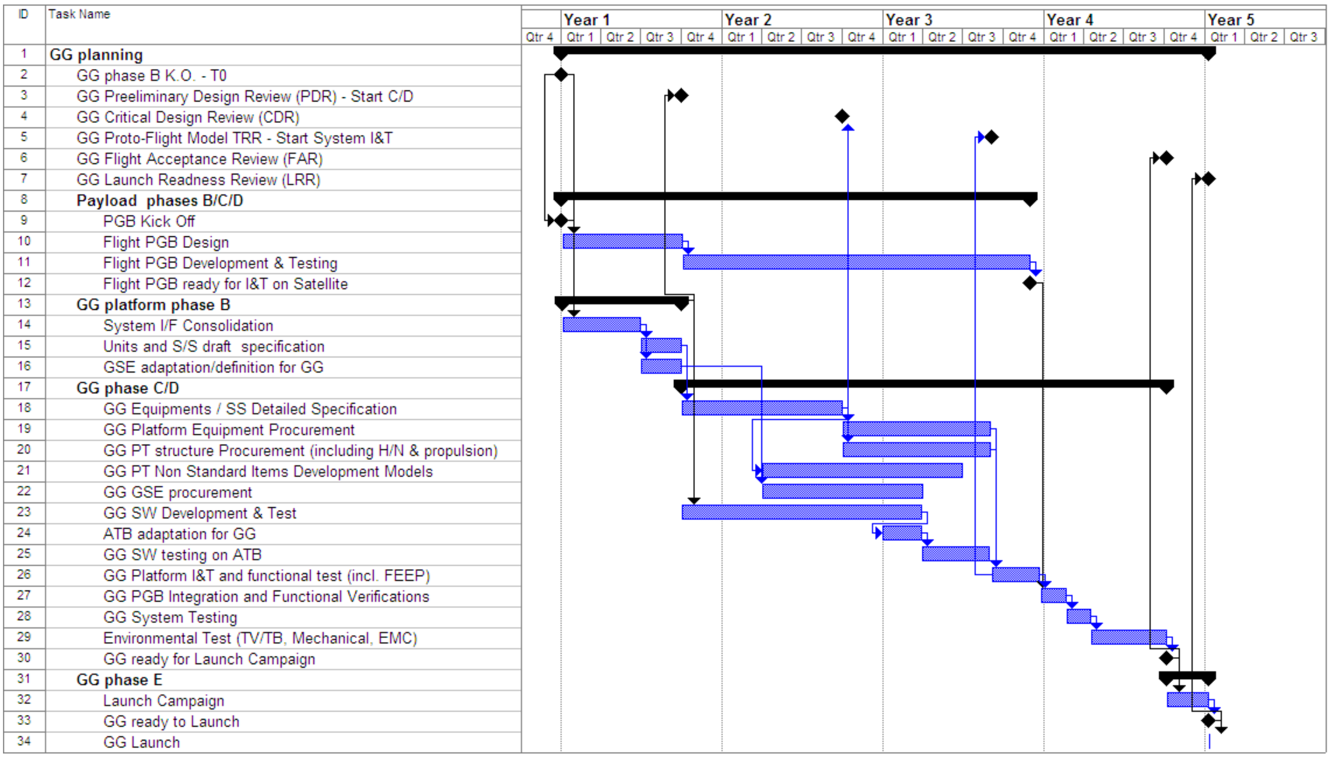

Figure 6.4-1: GG program master schedule

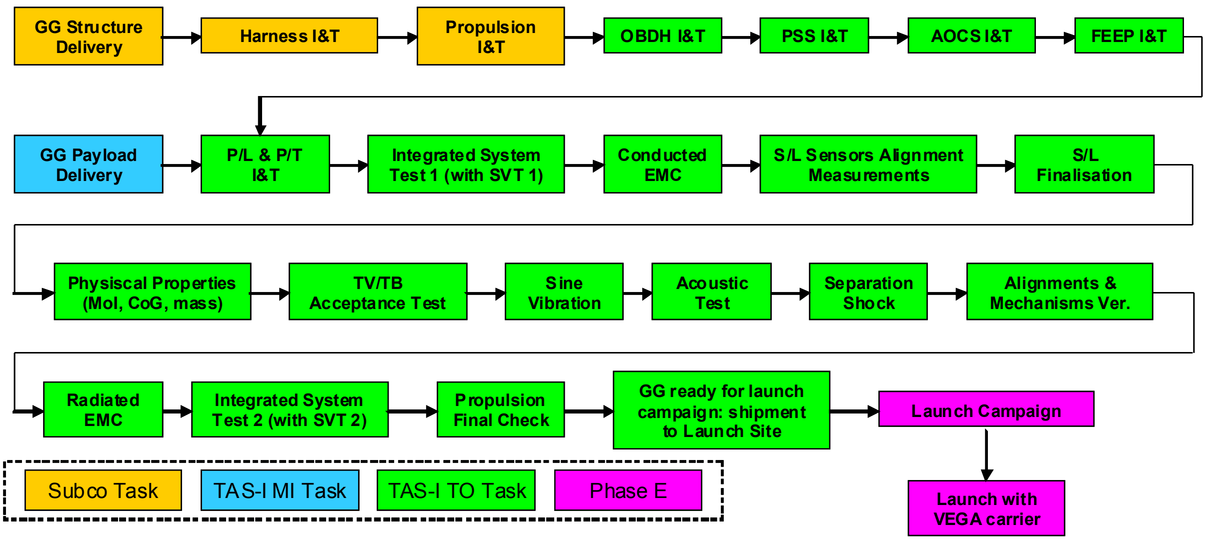

Figure 6.4-2: Satellite level test sequence

The project management plan is based on the assumption of a small dedicated project team at TAS-I Torino, providing all system engineering and managing procurement of the hardware items. The project team has a counterpart at TAS-I Milano providing parallel development of the payload module, in collaboration with the University of Pisa and INFN. Further assumptions, necessary to meet the cost objective, include:

- Maximum use of previously flown designs and components;
- Modular architecture allowing parallel development of different subsystems with well defined and robust interfaces;
- Maximum involvement of engineering resources with previous experience of projects with similar elements and objectives (e.g. GOCE);
- In-house development of application software;
- Direct involvement of subcontractor engineering resources in the project team;
- Technically competent project management;
- Well defined mission objectives and capacity for taking prompt decisions about mission implementation, in response to the evolving understanding of the mission requirements;
- Appropriate, streamlined documentation requirements.

8. ACRONYMS AND ABBREVIATIONS

AD	Applicable Document
AIV	Assembly Integration and Test
AOCS	Attitude and Control Subsystem
ASI	Agenzia Spaziale Italiana
BCR	Battery Charge Regulator
BDR	Battery Discharge Regulator
CDMU	Command and Data Management Unit
CDR	Critical Design Review
CFRP	Carbon Fiber Reinforced Plastics
CGPS	Cold Gas Propulsion System
CMRR	Common Mode Rejection Ratio
CNES	Centre National d'Etudes Spatiales
COG	Center of Gravity
COM	Center of Mass
CPE	Control and Processing Electronics
CPU	Central Processing Unit
DCAP	Dynamics and Control Analysis Package
DFACS	Drag Free and Attitude Control Subsystem
DFM	Drag Free Mode
DoD	Depth of Discharge
E2E	End To End Simulator
ECE	Experiment Control Electronics
ECSS	European Cooperation for Space Standardization
EGSE	Electrical Ground Support Equipment
EMC	Electromagnetic Compatibility
EOL	End of Life
EP	Equivalence Principle
EPS	Electrical Power System
EQM	Engineering Qualification Model
ESA	European Space Agency
FAR	Flight Acceptance Review
FDIR	Failure Detection Isolation and Recovery
FEEP	Field Emission Electric Propulsion
FEM	Finite Element Model
FOV	Field of View
G/S	Ground Station
GG	Galileo Galilei (Satellite)
GGG	Galileo Galilei on the Ground (Experiment)
GOCE	Gravity and Ocean Circulation Explorer
HK	Housekeeping
I/F	Interface
HDPE	High Density Polyethylene
INFN	Istituto Nazionale di Fisica Nucleare
INRIM	Istituto Nazionale Ricerca Metrologica
IRF	Inertial Reference Frame
I&T	Integration & Test
LEOP	Launch and Early Orbit Phase
LGA	Low Gain Antenna
LHCO	Left Handed Circular Polarization
LRR	Launch Readiness Review
MLI	Multi Layer Insulation
MOI	Moment Of Inertia
MRD	Mission Requirement Document
MSIS	Mass Spectrometer and Incoherent Scatter
OBDH	On Board Data Handling
OCC	Operations Control Center
P/L	Payload
PA	Product Assurance
PCDU	Power Control and Distribution Unit
PCE	Payload Control Electronics
PCU	Power Control Unit
PDR	Preliminary Design Review
PFM	Protoflight Model
PGB	Pico Gravity Box
PRR	Preliminary Requirements Review
PSD	Position Sensing Detector
PSLV	Polar Satellite Launch Vehicle
RD	Reference Document
RFDN	Radiofrequency Distribution Network
RHCP	Right Handed Circular Polarization
SA	Solar Array
SD	Standard Document
S/C	Spacecraft
SOC	Science Operations Center
SPF	Single Point Failure
S^3R	Sequential Switching Shunt Regulator
S/S	Subsystem
STM	Structural-Thermal Model
SVF	Software Validation Facility
TAS-I	Thales Alenia Space Italia
TB	Thermal Balance
TBC	To Be Confirmed
TBD	To Be Defined
TC	Telecommand
TCS	Thermal Control System
TM	Telemetry
TM	Test Mass
TMM	Thermal Mathematical Model
TRL	Technology Readiness Level
TT&C	Tracking Telemetry & Command
TV	Thermal Vacuum

CONTROLLED DISTRIBUTION

9. REFERENCES

9.1 Applicable Documents

[AD 1] ASI, “Progetto Galileo Galilei-GG Fase A-2, Capitolato Tecnico”, DC-IPC-2007-082, Rev. B, 10-10-2007 and applicable documents defined therein

9.2 ASI Reference Documents

[RD 1] GG Phase A Study Report, Nov. 1998, revised Jan. 2000, available at: http://eotvos.dm.unipi.it/nobili/ggweb/phaseA/index.html

[RD 2] Supplement to GG Phase A Study (GG in sun-synchronous Orbit) “Galileo Galilei-GG”: design, requirements, error budget and significance of the ground prototype”, A.M. Nobili et al., Physics Letters A 318 (2003) 172–183, available at: http://eotvos.dm.unipi.it/nobili/documents/generalpapers/GG_PLA2003.pdf

[RD 3] A. Nobili, GG Science Requirements, Pisa, September 2008

9.3 GG Phase A2 Study Notes

[RD 4] SD-RP-AI-0625, GG Final Report / Satellite Detailed Architecture Report, Issue 1

[RD 5] SD-RP-AI-0626, GG Phase A2 Study Executive Summary, Issue 1

[RD 6] SD-TN-AI-1163, GG Experiment Concept and Requirements Document, Issue 3

[RD 7] SD-RP-AI-0620, GG System Performance Report, Issue 2

[RD 8] SD-TN-AI-1167, GG Mission Requirements Document, Issue 2

[RD 9] SD-RP-AI-0590, GG System Concept Report (Mission Description Document), Issue 3

[RD 10] SD-SY-AI-0014, GG System Functional Specification and Preliminary System Technical Specification, Issue 1

[RD 11] SD-RP-AI-0631, GG Consolidated Mission Description Document, Issue 1

[RD 12] SD-TN-AI-1168, GG Mission Analysis Report, Issue 2

[RD 13] GG-TN-DTM-002, Galileo Galilei Satellite - Design & Structural Analysis Report, Issue 1

[RD 14] SD-RP-AI-0627, GG Thermal Design and Analysis Report, Issue 1

[RD 15] SD-RP-AI-0268, GG System Budgets Report, Issue 1

[RD 16] SD-RP-AI-0621, Technical Report on Drag and Attitude Control, Issue 2

[RD 17] TL25033, Payload Architectures and Trade-Off Report, Issue 3

[RD 18] SD-RP-AI-0629, Technical Report on Simulators, Issue 1

[RD 19] GG.ALT.TN.2003, FEEP Microthruster System Technical Report, Issue 1

[RD 20] TASI-FI-44/09, Cold Gas Micro Thruster System for Galileo Galilei (GG) Spacecraft - Technical Report, Issue 1, May 2009

[RD 21] SD-RP-AI-0630, Spin Sensor Design, Development and Test Report, Issue 1

[RD 22] SD-TN-AI-1169, GG Launcher Identification and Compatibility Analysis Report, Issue 1

[RD 23] ALTEC-AD-001, GG Ground Segment Architecture and Design Report, Issue 1

[RD 24] SD-TN-AI-1218, GG Preliminary Product Tree, Issue 1

[RD 25] SD-PL-AI-0227, GG System Engineering Plan (SEP), Issue 2

[RD 26] TAS-I, Payload Development and Verification Plan, Issue 1

[RD 27] SD-PL-AI-0228, GG System Verification and Validation Plan, Issue 1

[RD 28] SD-TN-AI-1219, Report on Frequency Management Issues, Issue 1

[RD 29] SD-RP-AI-0632, GG Mission Risk Assessment And Mitigation Strategies Report, Issue 1

[RD 30] SD-RP-AI-0633, Report on Mission Cost Estimates, Issue 1

END OF DOCUMENT